Equivalent Polynomials for Heaviside function enriched elements

Internal Report

G.Ventura*

Politecnico di Torino, Corso Duca degli Abruzzi 24, 10129 Torino, Italy

SUMMARY

This internal report summarizes the background for the determination of Equivalent Polynomials allowing one-cell quadrature in Heaviside function enriched elements.

1. XFEM FORMULATION AND QUADRATURE WITH EQUIVALENT POLYNOMIALS.

The classical approximation to the displacement field in XFEM is given by the well-known expression [1, 2]

$$\mathbf{u}(\mathbf{x}) = \sum_{I \in \mathcal{N}} N_I(\mathbf{x}) \left(\mathbf{u}_I + \mathbf{a}_I f_{\mathrm{e}}(\mathbf{x}) \right) \tag{1}$$

where $\mathbf{u}$ is the displacement field, $\mathcal{N}$ are the nodes of the finite element mesh, $N_I(\mathbf{x})$ the finite element shape functions, f_{e} the enrichment function, $\mathbf{u}_I$ and $\mathbf{a}_I$ the standard and enrichment nodal variables, respectively.

In the present work the enrichment function will be assumed given by the generalized Heaviside step function, Fig. 1

$$f_{\mathrm{e}}(\mathbf{x}) = H(\mathbf{x}) = \mathrm{sign}\left(d(\mathbf{x})\right) = \begin{cases} 1 & \text{if} \quad d(\mathbf{x}) > 0 \\ -1 & \text{if} \quad d(\mathbf{x}) < 0 \end{cases} \tag{2}$$

This function describes a displacement jump at $d = 0$, so it is of general use when dealing with cracks in any number of dimensions. The enrichment part in (1) is added only to the nodes of the elements cut by the discontinuity, so that these elements are called enriched elements.

The discontinuous function (2), enriching the finite element space by (1), will then enter the element stiffness matrix, so that Gaussian quadrature cannot be used unless the element domain is split into two subdomains, one for each side of the discontinuity. This can be immediately observed by applying the virtual work principle for determining the element stiffness: here the derivation presented in [3, 4] is briefly recalled for introducing the notation used in this paper. Consider the restriction of the displacement and strain field in vector form to a single enriched finite element Ω_{e}

$$\mathbf{u} = \mathbf{N}\mathbf{u}_{\mathrm{e}} + H\mathbf{N}\mathbf{a}_{\mathrm{e}} \tag{3}$$

$$\boldsymbol{\varepsilon} = \mathbf{B}\mathbf{u}_{\mathrm{e}} + H\mathbf{B}\mathbf{a}_{\mathrm{e}} \tag{4}$$

*Correspondence to: Giulio Ventura, Politecnico di Torino - DISEG, Corso Duca degli Abruzzi 24, 10129 Torino, Italy. Email: giulio.ventura@polito.it

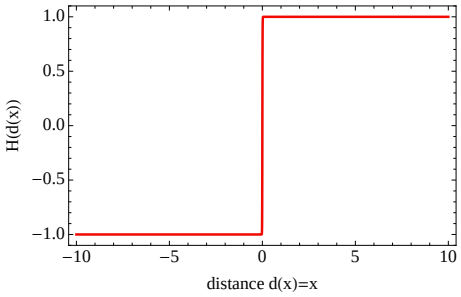

Figure 1. Enrichment function for crack problems.

where $\mathbf{u}_\mathrm{e}$, $\mathbf{a}_\mathrm{e}$ are the element standard and enriched nodal variables and $\nabla_{\boldsymbol{\varepsilon}}$ is the symmetric gradient operator, so that $\mathbf{B}\,\mathbf{u}_\mathrm{e} = (\nabla_{\boldsymbol{\varepsilon}}\mathbf{N})\;\mathbf{u}_\mathrm{e}$. In (4) the derivatives of H do not appear being zeroes.

Let $\mathbf{E}$ be the elastic operator, such that the stress $\boldsymbol{\sigma}$ is given by $\boldsymbol{\sigma} = \mathbf{E}\boldsymbol{\varepsilon}$. The element internal virtual work is given by

$$\begin{aligned} L_\mathrm{i} = \int_{\Omega_\mathrm{e}} \boldsymbol{\varepsilon}^\mathrm{T}\boldsymbol{\sigma}\,\mathrm{d}\Omega = \\ \int_{\Omega_\mathrm{e}} \mathbf{B}^\mathrm{T}\mathbf{E}\,\mathbf{B}\,\mathrm{d}\Omega\,\mathbf{u}_\mathrm{e}\cdot\mathbf{u}_\mathrm{e} + \int_{\Omega_\mathrm{e}} \left(H\mathbf{B}^\mathrm{T}\mathbf{E}\,\mathbf{B}\right)\,\mathrm{d}\Omega\,\mathbf{a}_\mathrm{e}\cdot\mathbf{u}_\mathrm{e} + \\ \int_{\Omega_\mathrm{e}} \left(H\mathbf{B}^\mathrm{T}\mathbf{E}\,\mathbf{B}\right)\,\mathrm{d}\Omega\,\mathbf{u}_\mathrm{e}\cdot\mathbf{a}_\mathrm{e} + \\ \int_{\Omega_\mathrm{e}} \left(H^2\mathbf{B}^\mathrm{T}\mathbf{E}\,\mathbf{B}\right)\,\mathrm{d}\Omega\,\mathbf{a}_\mathrm{e}\cdot\mathbf{a}_\mathrm{e} \end{aligned} \tag{5}$$

Consequently, considering that $H^2 = 1$, the element stiffness matrix is

$$\mathbf{K}_\mathrm{e} = \int_{\Omega_\mathrm{e}} \left[\begin{array}{c|c} \mathbf{B}^\mathrm{T}\mathbf{E}\,\mathbf{B} & H\mathbf{B}^\mathrm{T}\mathbf{E}\,\mathbf{B} \\ \hline H\mathbf{B}^\mathrm{T}\mathbf{E}\,\mathbf{B} & \mathbf{B}^\mathrm{T}\mathbf{E}\,\mathbf{B} \end{array}\right]\mathrm{d}\Omega \tag{6}$$

where the matrix has been partitioned into four submatrices according to the nodal variables $\mathbf{u}_\mathrm{e}$ and $\mathbf{a}_\mathrm{e}$. The stiffness matrix can be seen as the sum of a polynomial, Gauss integrable part, $\mathbf{K}_\mathrm{e}^{(\mathrm{p})}$ and a discontinuous part $\mathbf{K}_\mathrm{e}^{(\mathrm{d})}$ as follows

$$\mathbf{K}_\mathrm{e}^{(\mathrm{p})} = \int_{\Omega_\mathrm{e}} \left[\begin{array}{c|c} \mathbf{B}^\mathrm{T}\mathbf{E}\,\mathbf{B} & \mathbf{0} \\ \hline \mathbf{0} & \mathbf{B}^\mathrm{T}\mathbf{E}\,\mathbf{B} \end{array}\right]\mathrm{d}\Omega \tag{7}$$

$$\mathbf{K}_\mathrm{e}^{(\mathrm{d})} = \int_{\Omega_\mathrm{e}} \left[\begin{array}{c|c} \mathbf{0} & H\mathbf{B}^\mathrm{T}\mathbf{E}\,\mathbf{B} \\ \hline H\mathbf{B}^\mathrm{T}\mathbf{E}\,\mathbf{B} & \mathbf{0} \end{array}\right]\mathrm{d}\Omega \tag{8}$$

The integration of the discontinuous part $\mathbf{K}_\mathrm{e}^{(\mathrm{d})}$ is performed in the literature by splitting the integration domain into two parts Ω_e^1 and Ω_e^2 at the discontinuity, so that Gaussian quadrature can be applied on each subdomain. Alternatively, approaches based on the application of the Gauss-Green theorem to the two subdomains have been successfully used as well [5].

A procedure to recover the possibility of using Gaussian quadrature on the entire element domain has been suggested in [3]. It is based on introducing an equivalent polynomial function $\tilde{H}$ having the property that

$$\int_{\Omega_\mathrm{e}} \tilde{H}\mathbf{B}^\mathrm{T}\mathbf{E}\,\mathbf{B}\,\mathrm{d}\Omega = \int_{\Omega_\mathrm{e}^1} H\mathbf{B}^\mathrm{T}\mathbf{E}\,\mathbf{B}\,\mathrm{d}\Omega + \int_{\Omega_\mathrm{e}^2} H\mathbf{B}^\mathrm{T}\mathbf{E}\,\mathbf{B}\,\mathrm{d}\Omega \tag{9}$$

Once $\tilde{H}$ is determined it is

$$\mathbf{K}_{\mathrm{e}} = \int_{\Omega_{\mathrm{e}}} \left[\begin{array}{c|c} \mathbf{B}^{\mathrm{T}}\mathbf{E}\,\mathbf{B} & \tilde{H}\mathbf{B}^{\mathrm{T}}\mathbf{E}\,\mathbf{B} \\ \hline \tilde{H}\mathbf{B}^{\mathrm{T}}\mathbf{E}\,\mathbf{B} & \mathbf{B}^{\mathrm{T}}\mathbf{E}\,\mathbf{B} \end{array}\right] \mathrm{d}\Omega \tag{10}$$

Equation (10) is Gauss integrable, being each term polynomial. The derivation of $\tilde{H}$ for some finite elements has been carried out in [3]. Here it is recalled that, for (9) to hold, $\tilde{H}$ must be a polynomial whose degree is at least equal to the polynomial degree of the term $\mathbf{B}^{\mathrm{T}}\mathbf{E}\,\mathbf{B}$. As an example, for the linear triangular or tetrahedral element the term $\mathbf{B}^{\mathrm{T}}\mathbf{E}\,\mathbf{B}$ is constant, so the single Equation (9) suffices for the determination of $\tilde{H}$, which will be a constant depending on the location of the discontinuity. For the linear quadrilateral the shape functions are bilinear, so that the term $\mathbf{B}^{\mathrm{T}}\mathbf{E}\,\mathbf{B}$ is quadratic. Then, as the polynomial coefficients multiplying $\tilde{H}$ vary depending on the element stiffness entry, the equivalence (9) is to hold for all power terms up to two, i.e.

$$\int_{\Omega_{\mathrm{e}}} \tilde{H}\,\mathrm{d}\Omega = \int_{\Omega_{\mathrm{e}}^1} H\,\mathrm{d}\Omega + \int_{\Omega_{\mathrm{e}}^2} H\,\mathrm{d}\Omega \tag{11a}$$

$$\int_{\Omega_{\mathrm{e}}} \tilde{H}\xi\,\mathrm{d}\Omega = \int_{\Omega_{\mathrm{e}}^1} H\xi\,\mathrm{d}\Omega + \int_{\Omega_{\mathrm{e}}^2} H\xi\,\mathrm{d}\Omega \tag{11b}$$

$$\int_{\Omega_{\mathrm{e}}} \tilde{H}\eta\,\mathrm{d}\Omega = \int_{\Omega_{\mathrm{e}}^1} H\eta\,\mathrm{d}\Omega + \int_{\Omega_{\mathrm{e}}^2} H\eta\,\mathrm{d}\Omega \tag{11c}$$

$$\int_{\Omega_{\mathrm{e}}} \tilde{H}\xi\eta\,\mathrm{d}\Omega = \int_{\Omega_{\mathrm{e}}^1} H\xi\eta\,\mathrm{d}\Omega + \int_{\Omega_{\mathrm{e}}^2} H\xi\eta\,\mathrm{d}\Omega \tag{11d}$$

$$\int_{\Omega_{\mathrm{e}}} \tilde{H}\xi^2\,\mathrm{d}\Omega = \int_{\Omega_{\mathrm{e}}^1} H\xi^2\,\mathrm{d}\Omega + \int_{\Omega_{\mathrm{e}}^2} H\xi^2\,\mathrm{d}\Omega \tag{11e}$$

$$\int_{\Omega_{\mathrm{e}}} \tilde{H}\eta^2\,\mathrm{d}\Omega = \int_{\Omega_{\mathrm{e}}^1} H\eta^2\,\mathrm{d}\Omega + \int_{\Omega_{\mathrm{e}}^2} H\eta^2\,\mathrm{d}\Omega \tag{11f}$$

where ξ and η are the element parent coordinates. Therefore, for Equations (11) to hold simultaneously, it is assumed

$$\tilde{H}(\xi,\eta) = c_0 + c_1\xi + c_2\eta + c_3\xi\eta + c_4\xi^2 + c_5\eta^2 \tag{12}$$

where the six constants $c_0 \ldots c_5$ are determined by solving the linear system (11).

This implies that, in general, the use of the equivalent polynomial function allows to apply standard Gaussian quadrature the cost of doubling the polynomial degree of the integrand in (10) as the Heaviside function is replaced by a polynomial of the same degree of the original stiffness matrix integrand.

It is important to point out clearly that the equivalent polynomial $\tilde{H}$ is not an interpolation to the function H. The relation between an n degree equivalent polynomial and the original Heaviside function H for a fixed domain is given by the equivalence of the integrals of $\tilde{H}$ and H for every

monomial term up to the degree n. To fix the ideas we state the property and compute the equivalent polynomials in the one-dimensional case on the domain $\Omega = [0, 1]$. It must be

$$\int_\Omega \tilde{H}\,\mathrm{d}\Omega = \int_\Omega H\,\mathrm{d}\Omega \tag{13a}$$

$$\int_\Omega \tilde{H}x\,\mathrm{d}\Omega = \int_\Omega Hx\,\mathrm{d}\Omega \tag{13b}$$

$$\int_\Omega \tilde{H}x^2\,\mathrm{d}\Omega = \int_\Omega Hx^2\,\mathrm{d}\Omega \tag{13c}$$

$$\vdots \tag{13d}$$

$$\int_\Omega \tilde{H}x^n\,\mathrm{d}\Omega = \int_\Omega Hx^n\,\mathrm{d}\Omega \tag{13e}$$

Let $\delta \in \Omega$ the position of the discontinuity, so that $d(x) = x - \delta$. The following Figures 2, 3, 4 illustrate the plots of $\tilde{H}$ for the degrees $0...5$ at three positions of the discontinuity $\delta = 0.2,\ 0.5,\ 0.7$. It may be seen immediately that the graph of $\tilde{H}$ is visually unrelated to the graph of H, so that $\tilde{H}$ is not an interpolation to H. Note, finally, that the polynomial coefficients of $\tilde{H}$ are function of the position of the discontinuity. For example, the second degree equivalent polynomial for the one-dimensional case at hand is

$$\tilde{H} = 1 - 2\delta + \left(-2\delta^2 + 4\delta - 1\right) x + \left(-2\delta^3 + 3\delta^2 - \frac{1}{2}\right) x^2 \tag{14}$$

Equation (14) can be the basis for using, instead of equivalent polynomials, special variable weights Gauss quadrature rules according to the approach introduced by [6]. In this case the weights will be function of the position of the discontinuity and will be given by the values of the equivalent polynomial at the Gauss Points.

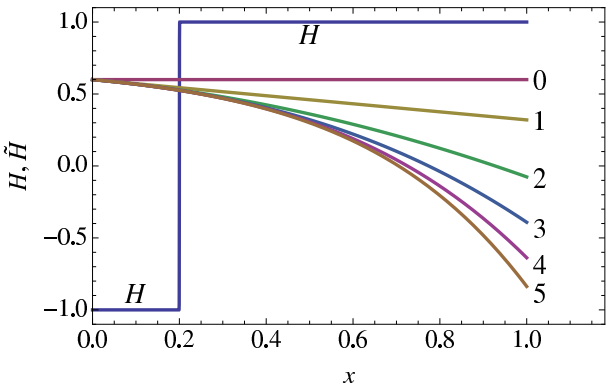

Figure 2. Graphs of H and the equivalent polynomials $\tilde{H}$ of degree $0...5$. The discontinuity is at $\delta = 0.2$. The number at the side of the curves is the degree of the equivalent polynomial.

2. DETERMINATION OF EQUIVALENT POLYNOMIALS

The equivalence formulas (9) or (11) rely on the fact that, for solving the problem of the determination of the equivalent polynomial, the two integrals on Ω_e^1 and Ω_e^2 are to be evaluated analytically for a general position of the discontinuity. This was accomplished by different techniques (including the use of the divergence theorem) in [3]. Equivalent polynomials for some

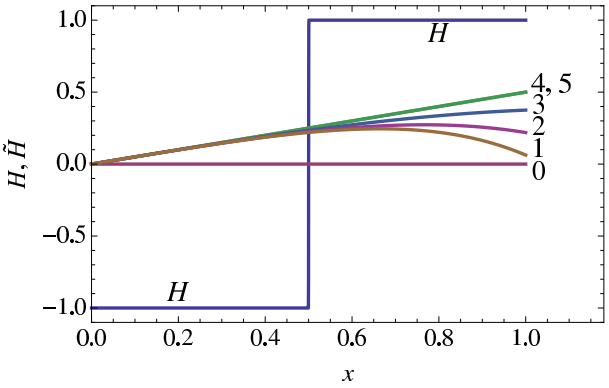

Figure 3. Graphs of H and the equivalent polynomials $\tilde{H}$ of degree $0...5$. The discontinuity is at $\delta = 0.5$. The number at the side of the curves is the degree of the equivalent polynomial.

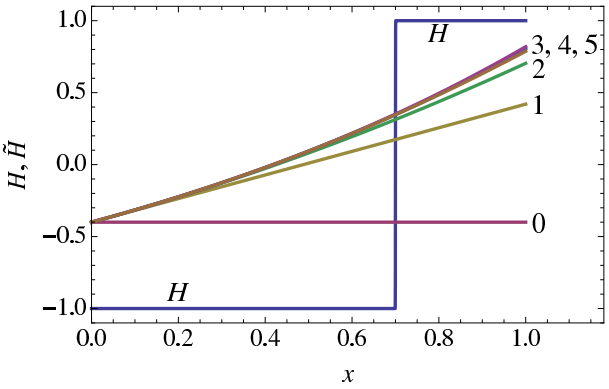

Figure 4. Graphs of H and the equivalent polynomials $\tilde{H}$ of degree $0...5$. The discontinuity is at $\delta = 0.7$. The number at the side of the curves is the degree of the equivalent polynomial.

important cases were given, e.g. bar, linear triangle, linear tetrahedron, linear quadrilateral. But some cases, for example the linear hexahedron, could not be practically solved due to the geometric complexity of the integration subregions in which the element is subdivided by an arbitrary position of the discontinuity. This was a serious limitation to the equivalent polynomials approach.

A radically different approach to the problem has been then developed to eliminate the complexity stemming from the non-standard shape of the integration subdomains. This new approach relies on the idea of replacing the Heaviside function with a regularized counterpart [7, 8], having the property of reverting to the original discontinuous function in the limit.

Consider the regularized form of the Heaviside function

$$H_\rho = \frac{2}{e^{-\rho x} + 1} - 1 \tag{15}$$

where e is the Euler's number and ρ is a regularization parameter. Some graphs of H_ρ are given in Figure 5. It can be observed that the discountinuous function H is reproduced as $\rho \to +\infty$. The motivation of introducing the regularized version of H is given by the fact that H_ρ is continuous and differentiable on $\mathbb{R}$ and its analytic primitive function is easily found.

Therefore, the equivalent polynomial $\tilde{H}_\rho$ to H_ρ can be determined in closed form by the formal equivalence relation

$$\int_{\Omega_e} \tilde{H}_\rho \mathcal{M}^{(i)} \, \mathrm{d}\Omega = \int_{\Omega_e} H_\rho \mathcal{M}^{(i)} \, \mathrm{d}\Omega \qquad i = 1 \dots m \tag{16}$$

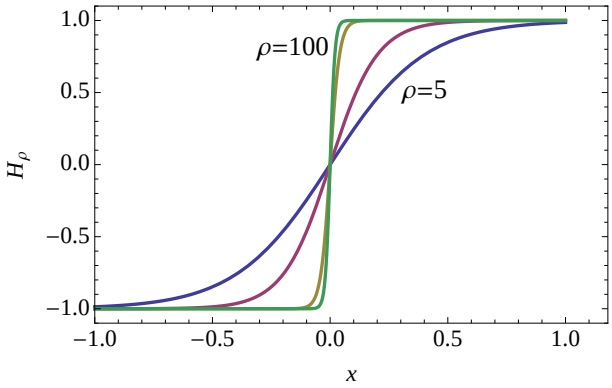

Figure 5. Graphs of H_ρ for increasing values of the regularization parameter ρ. As ρ diverges the regularized function graph reproduces the Heaviside function.

$\tilde{H}_\rho$ being the equivalent polynomial and $\mathcal{M}^{(i)}$ the monomial of degree i. Equations (16) are a system of m linear equations in the m unknown equivalent polynomial coefficients. Clearly, if n is the degree of the equivalent polynomial that it is to be computed, the number of monomials is $m = (n+1)$ in one dimension, $m = (n+1)(n+2)/2$ in two dimensions and $m = (n+1)(n+2)(n+3)/6$ in three dimensions.

Taking the limit of (16) for $\rho \to +\infty$ it is

$$\lim_{\rho\to\infty} \int_{\Omega_e} \tilde{H}_\rho \mathcal{M}^{(i)} \, \mathrm{d}\Omega = \lim_{\rho\to\infty} \int_{\Omega_e} H_\rho \mathcal{M}^{(i)} \, \mathrm{d}\Omega \qquad i = 1 \dots m \tag{17}$$

and applying the bounded convergence theorem the limit and integration operators can be "swapped", so that

$$\int_{\Omega_e} \lim_{\rho\to\infty} \tilde{H}_\rho \mathcal{M}^{(i)} \, \mathrm{d}\Omega = \int_{\Omega_e} \lim_{\rho\to\infty} H_\rho \mathcal{M}^{(i)} \, \mathrm{d}\Omega \qquad i = 1 \dots m \tag{18}$$

Being

$$\lim_{\rho\to\infty} H_\rho \mathcal{M}^{(i)} = H \mathcal{M}^{(i)} \qquad i = 1 \dots m \tag{19}$$

it is, by definition of equivalent polynomial and (17), (18)

$$\tilde{H} \mathcal{M}^{(i)} = \lim_{\rho\to\infty} \tilde{H}_\rho \mathcal{M}^{(i)} \qquad i = 1 \dots m \tag{20}$$

and then

$$\tilde{H} = \lim_{\rho\to\infty} \tilde{H}_\rho \tag{21}$$

Therefore, the equivalent polynomial $\tilde{H}$ can be computed by taking the limit for $\rho \to +\infty$ of $\tilde{H}_\rho$.

Consider, for the sake of illustration, the example one-dimensional case (13) introduced in the previous Section. Replacing H with H_ρ in (13) and solving, we obtain for the second degree equivalent polynomial the expression

$$\begin{aligned}\tilde{H}_\rho = \frac{1}{2\rho^3} \Big[& x^2 \left(12\rho \mathrm{Li}_2\left(-e^{-d\rho}\right) + 12\rho \mathrm{Li}_2\left(-e^{\rho-d\rho}\right) + 24\mathrm{Li}_3\left(-e^{-d\rho}\right) - 24\mathrm{Li}_3\left(-e^{\rho-d\rho}\right) + \rho^3\right) + \\ & + x\left(-8\rho \mathrm{Li}_2\left(-e^{-d\rho}\right) + 8\rho \mathrm{Li}_2\left(-e^{\rho-d\rho}\right) - 8\rho^2 \log\left(e^{(d-1)\rho}+1\right) + 8\rho^2 \log\left(e^{d\rho}+1\right) + \right. \\ & \left. + 8\rho^2 \log\left(e^{\rho-d\rho}+1\right) - 6\rho^3\right) + 4\rho^2 \log\left(e^{(d-1)\rho}+1\right) - 4\rho^2 \log\left(e^{d\rho}+1\right) + 2\rho^3 \Big]\end{aligned} \tag{22}$$

where $\mathrm{Li}_n(f)$ is the polylogarithm function of order n and argument f, defined as:

$$\mathrm{Li}_n(f) = \sum_{k=1}^{\infty} \frac{f^k}{k^n} \tag{23}$$

whose evaluation is possible through numerical libraries.

It may be easily verified that the graph of (22) reproduces its limit polynomial for $\rho \to \infty$ (14) for even very low values of ρ, Figure 6.

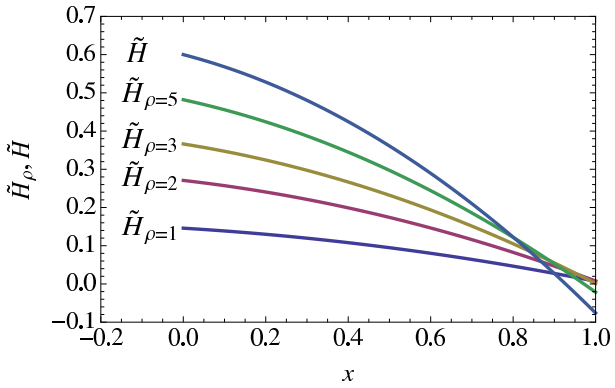

Figure 6. Graphs of the second degree equivalent polynomial $\tilde{H}_\rho$ for increasing values of the regularization parameter ρ and its limit function $\tilde{H}$.

2.1. Vector expression of equivalent polynomials

The equivalence equations (16) are formed by a left hand side with a polynomial integrand, that can be computed both in closed form or numerically, and a right hand side where the product of the regularized Heaviside function appear and that will be computed analytically. The equivalence is stated at the parent element level, so that the Jacobian related to the isoparametric mapping procedure does not appear. Its influence will be shown in Section 3. To get more compact results and improve efficiency it is advantageous to write the equivalence equations (16) in vector form [9]. Let

$$\tilde{H}_\rho = \mathbf{C} \cdot \boldsymbol{\mathcal{M}} \tag{24}$$

where $\boldsymbol{\mathcal{M}}$ collects the monomials $\mathcal{M}^{(i)}$, $i = 1 \dots m$, the symbol $\cdot$ is the scalar product between vectors and $\mathbf{C}$ is the vector of the m unknown coefficients to be determined defining the equivalent polynomial. With this notation (16) is written

$$\int_{\Omega_e} \boldsymbol{\mathcal{M}} \boldsymbol{\mathcal{M}}^{\mathrm{T}} \,\mathrm{d}\Omega\, \mathbf{C} = \int_{\Omega_e} H_\rho \boldsymbol{\mathcal{M}} \,\mathrm{d}\Omega \tag{25}$$

Let

$$\mathbf{A} = \int_{\Omega_e} \boldsymbol{\mathcal{M}} \boldsymbol{\mathcal{M}}^{\mathrm{T}} \,\mathrm{d}\Omega \tag{26}$$

$$\mathbf{b} = \int_{\Omega_e} H_\rho \boldsymbol{\mathcal{M}} \,\mathrm{d}\Omega \tag{27}$$

From (25)(26) (27) the determination of the constants $\mathbf{C}$ is done by solving the linear system

$$\mathbf{A}\mathbf{C} = \mathbf{b} \quad \Longrightarrow \quad \mathbf{C} = \mathbf{A}^{-1}\mathbf{b} \tag{28}$$

so that by (24)

$$\tilde{H}_\rho = \boldsymbol{\mathcal{M}}^{\mathrm{T}} \mathbf{A}^{-1} \mathbf{b} \tag{29}$$

Note that $\mathbf{A}$ is a matrix of constants for each element family (e.g. linear tetrahedron, hexahedron, ...) and degree of the equivalent polynomial. Its evaluation is possible by Gaussian quadrature, $\mathbf{A}$ being given by products of monomials.

The difficulty in the application of the approach is therefore concentrated in the evaluation of the vector $\mathbf{b}$ given by (27).

As previously evidenced, the use of a regularized counterpart to the Heaviside function allows to carry the integration in (27) without partitioning the domain. It is however not convenient (although possible) to evaluate (27) numerically as this operation would be expensive considering the high gradients of H_ρ as ρ becomes large to reproduce the discontinuous Heaviside function H, Figure 5.

Therefore, the evaluation of $\mathbf{b}$ is done in closed form for an arbitrary position of the discontinuity and value of the regularization parameter ρ. Several continuous and differentiable approximations to H have been tried, and the selection of the form (15) has been done as it is integrable in closed form and produces the shortest results.

In the application of the method the analytic expression of $\mathbf{b}$ is evaluated numerically at each enriched element for a reasonably high value of ρ and the equivalent polynomial is computed by (28) and (24).

In the next Section results are given for the linear tetrahedron and hexahedron, but they can be derived for elements of any order and dimensionality. The Appendix to this paper reports and briefly illustrates a formal Mathematica® code to compute the matrix $\mathbf{A}$ and the vector $\mathbf{b}$ given above in (26), (27).

2.2. *Practical use of the equivalent polynomial formulas*

It is useful to recap how the derived expressions for the equivalent polynomials can be used in practice. The following operative logical flow can be implemented:

1. for a given finite element the derivatives of the shape functions and the element stiffness is analyzed to produce the list of the monomials $\mathcal{M}$ appearing in the integration of the standard (non enriched) stiffness matrix. This can be done examining the product $\mathbf{B}^{\mathrm{T}}\mathbf{B}$ in (6), as $\mathbf{E}$ is a matrix of constants. Let n be the maximum monomial degree in $\mathcal{M}$;
2. once $\mathcal{M}$ is known, the matrix $\mathbf{A}$ can be immediately evaluated by standard Gauss quadrature in the element domain by (26). This integration will use the same number and location of quadrature points as in the standard, non enriched, finite element (being the polynomial degree of the integrand the same). The matrix $\mathbf{A}$ is factorized or inverted once for all in preparation of the system solution (28);
3. as the equivalent polynomial is defined as a linear combination (24) of the monomials in $\mathcal{M}$ and as it will multiply the term $\mathbf{B}^{\mathrm{T}}\mathbf{E}\mathbf{B}$ in (10), a suitable standard Gauss integration rule has to be introduced, accounting for the fact that the polynomial degree of the integrand will be $2n$;
4. the analytic expressions of the vector $\mathbf{b}$ are evaluated at each of the above Gauss points. At these points the values of $\tilde{H}$ are immediately computed by (29) for the numerical evaluation of (10).

2.3. *Accuracy of the equivalent polynomials*

The equivalent polynomials, being based on analytic integration and exact equivalence (16), do not introduce in principle any kind of approximation. However, there are two unavoidable sources of accuracy decrease. One is tied to the numerical error in the library used to compute the polylogarithms appearing in the solution [10, 11, 12] and the other is connected to the fact that a formal limit for the regularization parameter ρ is not evaluated, so that a suitable large value is used and an approximation is introduced. This value cannot be "too high" as this will produce elevate roundoff errors.

Table I. Approximation estimate for varying monomial degree n and regularization parameter ρ.

	$n=0$	$n=1$	$n=2$	$n=3$	$n=4$
$\rho=50$	2.8%	5.4%	7.9%	10.3%	12.6%
$\rho=100$	1.4%	2.7%	4.1%	5.3%	6.6%
$\rho=150$	0.9%	1.8%	2.7%	3.6%	4.5%
$\rho=200$	0.7%	1.4%	2.1%	2.7%	3.4%

Assume the numerical error in the evaluation of the polylogarithms is negligible. The correct order of magnitude for the regularization parameter ρ is determined in the following by a simplified but effective procedure. As seen in Figure 5, when the regularization parameter diverges the regularized function H_ρ graph tends to the exact Heaviside function. The error in the determination of the element stiffness does not stem from the punctual difference $H - H_\rho$ between the exact and the regularized function, but rather from the difference in their integrals. Moreover, the error will be largest for the highest degree monomial terms in the integrand when these terms will have their maximum at the discontinuity as detailed in the following.

To get an estimate of the error, consider the one dimensional case and assume the discontinuity be located at $\xi = 0$ in the parent element domain $[0, 1]$. Let $w_n(\xi)$ a monomial weight function of degree n. It is

$$I_e(n) = \int_0^1 w_n(\xi) H(\xi)\, \mathrm{d}\xi \tag{30}$$

$$I_\rho(n) = \int_0^1 w_n(\xi) H_\rho(\xi)\, \mathrm{d}\xi \tag{31}$$

where $I_e(n)$ and $I_\rho(n)$ are the exact and approximated integral depending on the weight function degree. The quadrature error in using the regularization is

$$\mathcal{E}_I(n) = \left| \frac{I_e(n) - I_\rho(n)}{I_e(n)} \right| \tag{32}$$

As the regularized Heaviside function rapidly assume the value of the exact function with the distance from the discontinuity, for the error to be maximum the monomial terms must have their maximum values at the discontinuity. Being the discontinuity at $\xi = 0$ the monomial terms to be considered in the error estimation are $w_n(\xi) = (1 - \xi)^n$. The error is observed maximum for the highest monomial degree. Table I reports the approximation error for several values of the regularization parameter ρ and the monomial degree n, while Figure 7 illustrates the graph of the approximation error with varying ρ for $n = 4$. It can be seen that, in practical applications, a value $\rho \simeq 200$ is sufficient to limit the approximation error to 3%.

3. EFFECT OF ISOPARAMETRIC MAPPING

In the present Section the effect of isoparametric mapping is studied and the concept of higher degree equivalent polynomial is introduced. The limiting case $\rho \to +\infty$ is considered.

When an element is distorted and isoparametric mapping is used, sources of numerical error arise. These are connected with the fact that the integrand in the stiffness evaluation changes from a polynomial to a rational function and that the discontinuity is distorted by the mapping. These fundamental aspects of XFEM application are not investigated in the literature, but the associated approximation in the evaluation of the element stiffness is not negligible. This approximation may be acceptable in some problems (e.g. linear elastic fracture mechanics, where the edges of the crack are not loaded) but can be a source of error in some applications like cohesive cracks and hydraulic fracture.

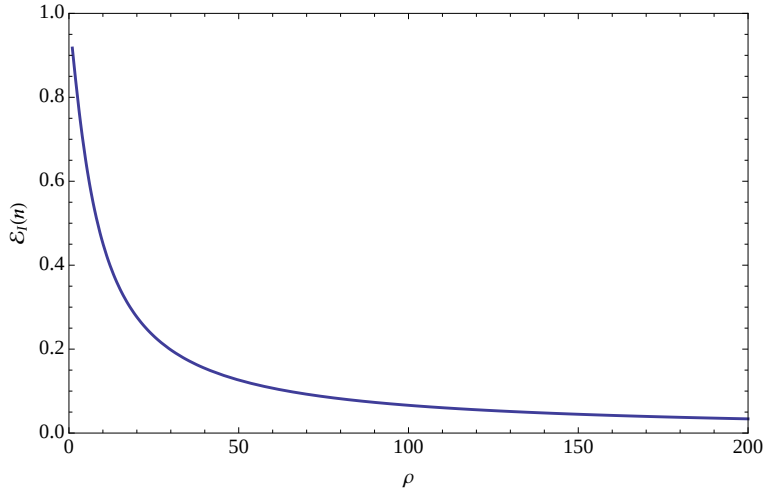

Figure 7. Approximation error for varying regularization parameter ρ and 4^{th} degree monomials.

In the present case an additional source of error may be present, originated by the fact that the equivalent polynomials are computed in the element parent domain, without accounting for the effect of the coordinate transformation.

A first study on this problem was presented in [3]. Then, it was realized that the way for measuring the error (the comparison of the values of the elements in the stiffness matrix) was not physically expressive and that some other aspects in the analysis should be further improved. Here that analysis is therefore briefly recalled, improved and expanded to get a much deeper insight on the problem and get a precise picture of its extent.

It has been pointed out that, in general, quadrature at the element level is performed in the parent domain by the well known isoparametric mapping, where the element global and parent reference frames are linked by a coordinate transformation.

In linear quadrilateral and hexahedral elements, when the opposite sides are non parallel, the inverse of the Jacobian is a rational function so that the integrand for the element stiffness evaluation is no longer polynomial. The traditional element Gaussian quadrature is therefore approximate and the proposed equivalent polynomial approach, exact for constant Jacobian, yields an approximate element stiffness matrix as well. Moreover, straight cracks are mapped to curved cracks in the parent element domain, introducing a new source of integration error even when element subdivision into quadrature subcells is used. Three sources of error are therefore into play

- element distortion
- discontinuity surface distortion
- approximate evaluation of the equivalent polynomial

These three aspects will be investigated in the following Section with reference to quadrilateral elements.

3.1. Distorted quadrilateral elements.

When computing the element stiffness for the quadrilateral element, a (2×2) Gauss point rule is usually chosen so to give exact quadrature in the parent domain. The fact that this quadrature rule is not exact for distorted elements due to the non-constant determinant of the Jacobian and the rational function structure of the integrand is commonly accepted [13]. The order of magnitude of this error will be given in the following.

When enriching a distorted the element with the Heaviside function for representing a jump discontinuity, the shape of the discontinuity surface is altered by the isoparametric mapping. Two

examples are given in Figs. 8 and 9, where it is shown how, when the element has non-parallel opposite sides, a straight discontinuity line in the element domain maps to a curve in the parent domain and vice-versa.

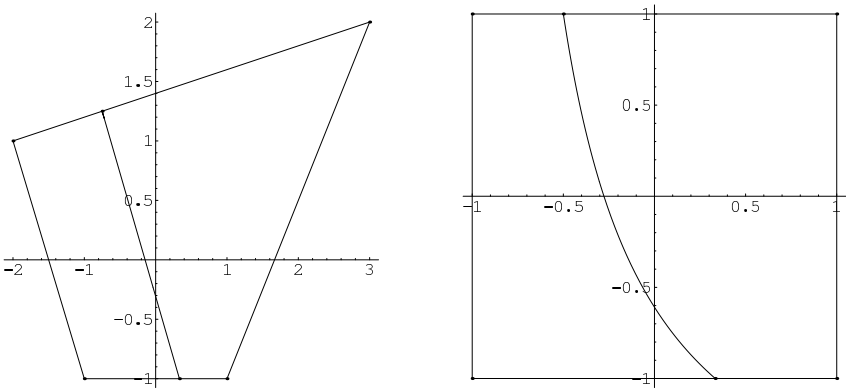

(a) (b)

Figure 8. Mapping of a line from a distorted element (a) to the parent domain (b).

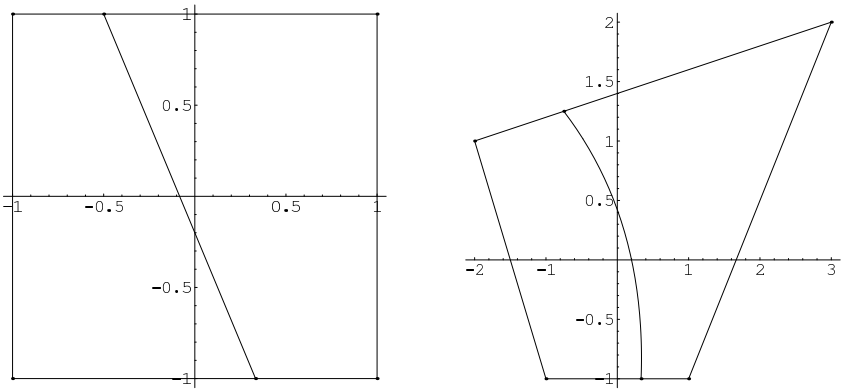

(a) (b)

Figure 9. Mapping of a line from the parent domain (a) to the distorted element domain (b).

As observed in [3], in the evaluation of the stiffness matrix by quadrature on subcells two approaches are therefore possible:

1. to assume a straight discontinuity line in the element domain and consider the two parts in which the element is split as quadrature subcells that will have then their own mappings for quadrature;
2. to assume a straight discontinuity line in the parent domain and define the two quadrature subcells in this reference.

Note that, if the first approach is used on a standard element (without enrichment), by arbitrarily splitting the element into two parts and then adding the stiffnesses computed in the two subcells, an error is observed as this sum will not be equal to the stiffness matrix computed on the entire element. This does not happen with the second approach where, if the contributions of the two quadrature subcells are added, the result coincides with the stiffness of the entire element.

Table II. Distorted quadrilaterals considered for errors computation. The columns report the vertexes coordinates V1...V4.

Label	V1	V2	V3	V4
Q1	$(+1,-1)$	$(+3,+2)$	$(-2,+1)$	$(-1,-1)$
Q2	$(+3,-1)$	$(+6,+2)$	$(-5,+1)$	$(-3,-1)$

Note that, in the use of equivalent polynomials, the second approach is adopted as the polynomial equivalence (16) is stated in the element parent domain. However, classical XFEM/GFEM literature employs the first approach.

Therefore, two sources of error are present in every XFEM/GFEM implementation applied to distorted elements: the error generated by the rational integrand and the error generated by combining the rational integrand with the Heaviside function.

The element stiffness is formed by four sub matrices (6),(10). We will focus on the discontinuous part of the element stiffness (6) that is

$$\mathbf{K}_{\mathrm{e}(12)} = \int_{\Omega_{\mathrm{e}}} H\mathbf{B}^{\mathrm{T}}\mathbf{E}\,\mathbf{B}\,\mathrm{d}\Omega \tag{33}$$

To study the influence of the various factors pointed out, four cases of distorted quadrilateral elements are considered, and the stiffness matrix is computed in the following cases:

1. element without crossing discontinuity line (to look at the influence of the distortion only);
   (a) by adaptive numerical quadrature (exact value);
   (b) by standard 2×2 Gauss quadrature;
2. element with crossing discontinuity;
   (a) by adaptive numerical quadrature (exact value);
   (b) by standard 2×2 Gauss quadrature applied to the two quadrature subcells in which the element is split;
   (c) by 3×3 Gauss quadrature introducing the equivalent polynomial $\tilde{H}$. The order of quadrature is increased as the use of equivalent polynomials doubles the degree of the integrand function [3].

While in Reference [3] the error in some of the above cases was computed as sup norm in between the elements of the stiffness matrix, with the consequence that the results may be misleading especially for the smallest values, here a different approach is considered. As the important factor is the strain energy stored inside the finite element, once the stiffness matrix is computed its eigenvalues are evaluated and a percentage error is given comparing the difference between the eigenvalues compared to the largest. More precisely, let $\lambda_i^{\mathrm{exact}}$ the eigenvalues of the stiffness matrix computed by adaptive quadrature sorted in descending order and $\lambda_i^{\mathrm{approx}}$ the same eigenvalues computed by one of the above methods (fixed points Gauss rule or equivalent polynomial). The percentage error in the i-th eigenvalues is defined by

$$\mathcal{E}_i = 100\frac{|\lambda_i^{\mathrm{approx}} - \lambda_i^{\mathrm{exact}}|}{\lambda_1^{\mathrm{exact}}} \tag{34}$$

where it is to be noted that for any i the largest eigenvalue, $\lambda_1^{\mathrm{exact}}$, always appears at the denominator.

For evaluating the errors introduced by the above sources we consider the two distorted quadrilaterals whose vertexes are listed in Table II and plotted in Fig.10. The two quadrilaterals are chosen one to have a strong non-parallelism between the opposite sides (Q1) and the other for being with a high elongation (Q2).

For the discontinuity inside the elements two cases are considered, labeled (a) and (b), respectively. In both cases the discontinuity line will cross two opposite element sides and it will have negative slope in case (a) and positive slope in case (b).

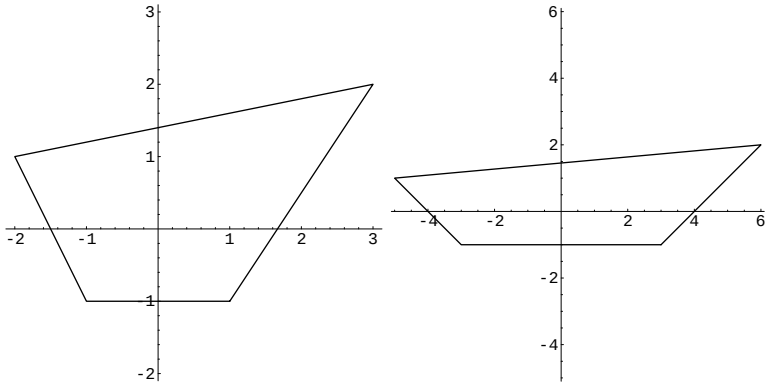

(a) (b)

Figure 10. Distorted quadrilaterals for error computations: (a) Q1; (b) Q2.

Table III. Errors in the stiffness eigenvalues due to element distortion and standard Gauss 2×2 quadrature rule. No discontinuity is considered.

Element	Eigenvalue	Percentage error $\mathcal{E}_i$
Q1	1	-0.13%
Q1	2	-0.29%
Q1	3	-1.27%
Q1	4	-0.80%
Q1	5	-1.18%
Q1	6	-0.05%
Q1	7	+0.00%
Q1	8	+0.00%
Q2	1	-0.04%
Q2	2	-0.14%
Q2	3	-0.37%
Q2	4	-0.84%
Q2	5	-0.07%
Q2	6	-0.00%
Q2	7	+0.00%
Q2	8	-0.00%

The intersection points $\mathbf{P}_1$ and $\mathbf{P}_2$ of the discontinuity in the parent coordinate system have coordinates $\mathbf{P}_1 = (4/5, -1)$, $\mathbf{P}_2 = (-3/4, +1)$ for case (a) and $\mathbf{P}_1 = (-4/5, -1)$, $\mathbf{P}_2 = (+3/4, +1)$ for case (b), Fig. 11. As previously pointed out, the discontinuity is assumed a line in the parent coordinate system, so that it is a curve in the physical domain.

Therefore, four situations will be considered, Q1(a), Q1(b), Q2(a) and Q2(b). The shape of the elements and the position of the discontinuity line have been chosen to be in between the worst error cases.

Table III lists the eigenvalues errors for the elements Q1 and Q2. No discontinuity is considered inside the elements and, as pointed out previously, the error arises from the 2×2 Gauss quadrature applied to the distorted elements, having rational stiffness integrand. The exact eigenvalues are computed by adaptive quadrature and it can be observed that the error is small and always less than 2%. Ideally, when the discontinuity line is introduced, it would be desirable the error to remain the same order of magnitude.

To investigate this, consider the discontinuity line and apply traditional subcells quadrature. The parent domain of the elements is subdivided into two quadrature subcells separated by the

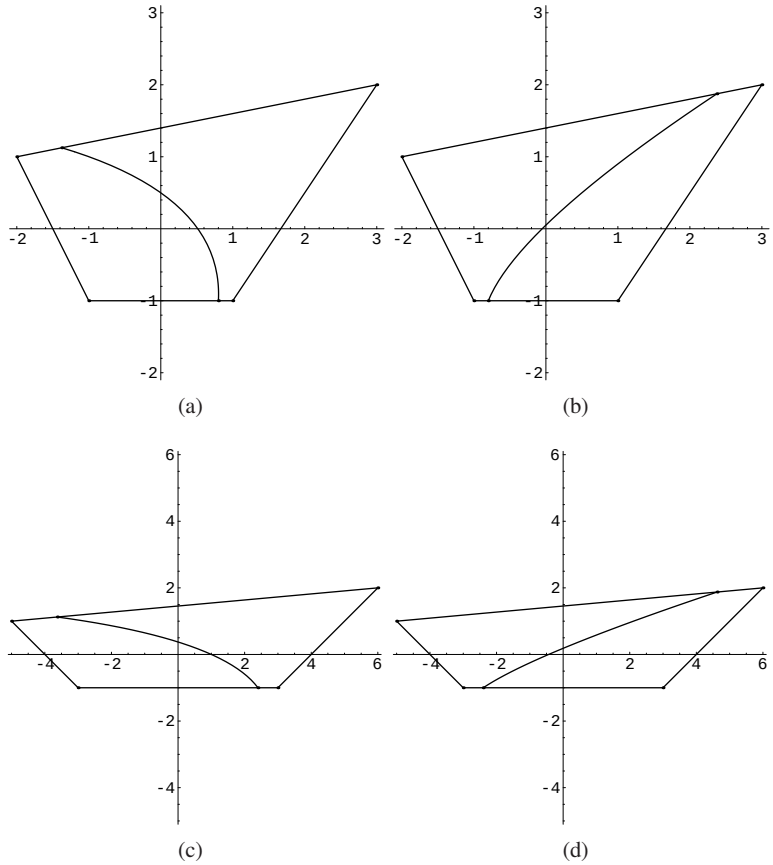

Figure 11. Distorted quadrilateral elements with discontinuity lines: (a) Case Q1(a), (b) Case Q1(b), (c) Case Q2(a), (d) Case Q2(b).

discontinuity line. Then 2×2 Gauss quadrature is applied to each subcells, while the exact stiffness is computed by adaptive quadrature. Tables IV, V reports the eigenvalues errors in the four examined cases Q1(a), Q1(b), Q2(a), Q2(b).

From Tables IV, V it can be seen that, in enriched distorted quadrilateral elements, the common practice of the quadrature on subcells introduces an error in the evaluation of the stiffness matrix that is commonly overlooked. The eigenvalue error can be the order of magnitude of 100%, i.e. much larger than that of non-enriched distorted elements.

The influence of the polynomial mapping is studied with the same technique. The equivalent polynomial $\tilde{H}$ is used for single cell quadrature in the evaluation of the stiffness matrix by (10). A 3×3 Gauss quadrature is used, being the degree of the polynomial integrand equal to 4. With these premises, Tables VI, VII report the percentage eigenvalues errors for the examined cases.

From the results it appears quite evident that polynomial mapping has several advantages:

- the element is not split into quadrature subcells;
- the eigenvalues error is much inferior compared to quadrature on subcells: it decreases from a maximum of 94% (Table IV) to a maximum of 3% (Table VI). The order of magnitude of the error is therefore the same as traditional non-enriched distorted elements, see Table III. Note that this result contradicts apparently what reported in Reference [3] but, as pointed out before, the sup norm in between the elements of the stiffness matrix yields misleading results because of the differences in the vanishing elements of the matrix;

Table IV. Element Q1. Errors in the stiffness eigenvalues due to element distortion and standard Gauss 2×2 quadrature rule on the two subcells generated by the discontinuity line.

Element	Discont. line	Eigenvalue	Percentage error $\mathcal{E}_i$
Q1	(a)	1	-0.35%
Q1	(a)	2	-1.07%
Q1	(a)	3	-93.9%
Q1	(a)	4	+87.3%
Q1	(a)	5	+0.03%
Q1	(a)	6	-0.19%
Q1	(a)	7	+0.00%
Q1	(a)	8	+0.00%
Q1	(b)	1	-1.21%
Q1	(b)	2	-0.73%
Q1	(b)	3	-1.94%
Q1	(b)	4	-1.83%
Q1	(b)	5	-0.11%
Q1	(b)	6	-0.09%
Q1	(b)	7	-0.00%
Q1	(b)	8	+0.00%

Table V. Element Q2. Errors in the stiffness eigenvalues due to element distortion and standard Gauss 2×2 quadrature rule on the two subcells generated by the discontinuity line.

Element	Discont. line	Eigenvalue	Percentage error $\mathcal{E}_i$
Q2	(a)	1	+0.91%
Q2	(a)	2	+0.36%
Q2	(a)	3	-77.8%
Q2	(a)	4	+77.0%
Q2	(a)	5	+0.03%
Q2	(a)	6	-0.00%
Q2	(a)	7	+0.00%
Q2	(a)	8	-0.00%
Q2	(b)	1	+0.32%
Q2	(b)	2	-0.05%
Q2	(b)	3	+0.57%
Q2	(b)	4	+0.29%
Q2	(b)	5	+0.01%
Q2	(b)	6	+0.01%
Q2	(b)	7	-0.00%
Q2	(b)	8	+0.00%

- the total number of Gauss points used in quadrature on subcells (2 subcells with 2×2 Gauss rule) and polynomial mapping (3×3 Gauss rule) is of the same order of magnitude, so no significant extra computational cost is involved.

The results of the proposed polynomial mapping technique are therefore interesting. Moreover, it has been verified that they can be further improved by increasing the degree of the equivalent polynomial as described in the following.

To this end it is important to recall again the meaning of defining the equivalent polynomial. This concept is related in some way to polynomial interpolation: given a polynomial integrand of degree n times the enrichment function, the equivalent polynomial is defined by the property of having the same integral on the parent element domain as the original integrand. Because of the linearity of the integral operator, this condition is equivalent to say that the equivalence property must hold for

each monomial term. This yielded n conditions so an equivalent polynomial of degree n is naturally defined. To match the number of equations and unknowns the degree of the equivalent polynomial cannot be different from n: it basically interpolates the result.

The same path of reasoning can be applied to a non-polynomial integrand, like the one arising in distorted elements. In this case, the conceptual meaning of the system of equations defining the equivalent polynomial is different, as it will approximate (and not interpolate) the result. If we think of the power expansion of the integrand, the equivalent polynomial realizes the exact integration of the terms of the expansion up to any chosen order n. Systems of equations of the kind (16) can be written up to any polynomial degree and the resulting equivalent polynomial gives an approximate solution to the quadrature problem. Note again that the equivalence equations are written always in the parent domain of the element, so that the Jacobian never enters the computation.

Table VI. Element Q1. Errors in the stiffness eigenvalues due to element distortion and polynomial mapping of the generalized Heaviside enrichment function.

Element	Discont. line	Eigenvalue	Percentage error $\mathcal{E}_i$
Q1	(a)	1	+1.24%
Q1	(a)	2	-0.08%
Q1	(a)	3	+2.88%
Q1	(a)	4	+1.29%
Q1	(a)	5	+0.22%
Q1	(a)	6	+0.07%
Q1	(a)	7	+0.00%
Q1	(a)	8	+0.00%
Q1	(b)	1	+2.50%
Q1	(b)	2	-1.52%
Q1	(b)	3	+1.53%
Q1	(b)	4	+1.20%
Q1	(b)	5	+0.31%
Q1	(b)	6	-0.28%
Q1	(b)	7	-0.00%
Q1	(b)	8	+0.00%

Table VII. Element Q2. Errors in the stiffness eigenvalues due to element distortion and polynomial mapping of the generalized Heaviside enrichment function.

Element	Discont. line	Eigenvalue	Percentage error $\mathcal{E}_i$
Q2	(a)	1	-0.59%
Q2	(a)	2	-0.93%
Q2	(a)	3	+0.75%
Q2	(a)	4	+0.37%
Q2	(a)	5	-0.07%
Q2	(a)	6	-0.01%
Q2	(a)	7	+0.00%
Q2	(a)	8	-0.00%
Q2	(b)	1	+1.67%
Q2	(b)	2	+0.95%
Q2	(b)	3	-0.14%
Q2	(b)	4	-0.47%
Q2	(b)	5	+0.05%
Q2	(b)	6	-0.02%
Q2	(b)	7	-0.00%
Q2	(b)	8	+0.00%

Table VIII. Element Q1. Errors in the stiffness eigenvalues due to element distortion and polynomial mapping of the generalized Heaviside enrichment function. Third degree equivalent polynomial.

Element	Discont. line	Eigenvalue	Percentage error $\mathcal{E}_i$
Q1	(a)	1	-0.19%
Q1	(a)	2	-0.01%
Q1	(a)	3	-0.16%
Q1	(a)	4	-0.02%
Q1	(a)	5	-0.03%
Q1	(a)	6	+0.01%
Q1	(a)	7	+0.00%
Q1	(a)	8	+0.00%
Q1	(b)	1	-0.07%
Q1	(b)	2	-0.01%
Q1	(b)	3	-0.10%
Q1	(b)	4	-0.03%
Q1	(b)	5	-0.03%
Q1	(b)	6	-0.01%
Q1	(b)	7	-0.00%
Q1	(b)	8	+0.00%

Table IX. Element Q2. Errors in the stiffness eigenvalues due to element distortion and polynomial mapping of the generalized Heaviside enrichment function. Third degree equivalent polynomial.

Element	Discont. line	Eigenvalue	Percentage error $\mathcal{E}_i$
Q2	(a)	1	-0.05%
Q2	(a)	2	+0.00%
Q2	(a)	3	-0.05%
Q2	(a)	4	+0.00%
Q2	(a)	5	+0.00%
Q2	(a)	6	+0.00%
Q2	(a)	7	+0.00%
Q2	(a)	8	-0.00%
Q2	(b)	1	+0.00%
Q2	(b)	2	+0.01%
Q2	(b)	3	+0.00%
Q2	(b)	4	+0.04%
Q2	(b)	5	+0.00%
Q2	(b)	6	+0.00%
Q2	(b)	7	-0.00%
Q2	(b)	8	+0.00%

To verify the effectiveness of this approach consider the problem of the distorted quadrilaterals and the third degree equivalent polynomial

$$\tilde{H} = c_0 + c_1\,\xi + c_2\,\eta + c_3\,\xi\,\eta + c_4\,\xi^2 + c_5\,\eta^2 + c_6\,\xi\,\eta^2 + c_7\,\eta\,\xi^2 + c_8\,\xi^3 + c_9\,\eta^3 \qquad (35)$$

By writing and solving the equivalence equations up to third order, the coefficients $c_0 \ldots c_9$ have been determined. Tables VIII, IX report the obtained results. Note that in this case the maximum polynomial degree of the integrand becomes 6, so that a 4×4 Gauss rule is required.

The results of Tables VIII, IX fully confirm the predicted result. In fact the eigenvalues error decreases to less than 0.2% and is therefore one order of magnitude less than the error of the simply distorted (non-enriched) element and three orders of magnitude less than quadrature on subcells.

This result non only demonstrates a further advantage of the polynomial mapping technique, but opens new perspectives for the reduction of quadrature errors in general finite element technology, whenever the stiffness matrix integrands are not polynomial functions.

REFERENCES

1. Belytschko T, Gracie R, Ventura G. A review of extended/generalized finite element methods for material modeling. *Modelling and Simulation in Materials Science and Engineering* 2009; **17**(4):043 001.
2. Fries TP, Belytschko T. The extended/generalized finite element method: An overview of the method and its applications. *International Journal for Numerical Methods in Engineering* 2010; **84**(3):253–304.
3. Ventura G. On the elimination of quadrature subcells for discontinuous functions in the extended finite-element method. *International Journal for Numerical Methods in Engineering* 2006; **66**:761–795.
4. Ventura G, Benvenuti E. Equivalent polynomials for quadrature in heaviside function enriched elements. *International Journal for Numerical Methods in Engineering* 2015; **102**:688–710.
5. Sudhakar Y, Wall WA. Quadrature schemes for arbitrary convex/concave volumes and integration of weak form in enriched partition of unity methods. *Computer Methods in Applied Mechanics and Engineering* 2013; **258**:39 – 54.
6. Holdych DJ, Noble DR, Secor RB. Quadrature rules for triangular and tetrahedral elements with generalized functions. *International Journal for Numerical Methods in Engineering* 2008; **73**(9):1310–1327.
7. Benvenuti E, Tralli A, Ventura G. A regularized xfem model for the transition from continuous to discontinuous displacements. *International Journal for Numerical Methods in Engineering* 2008; **74**(6):911–944.
8. Benvenuti E, Ventura G, Ponara N, Tralli A. Variationally consistent extended fe model for 3d planar and curved imperfect interfaces. *Computer Methods in Applied Mechanics and Engineering* 2013; **267**:434 – 457.
9. Esnault J. étude expérimental et numérique 3d du développement en fatigue d'une fissure déversée dans une tôle mince mtallique. PhD Thesis, Ecole Polytechnique, France 2014.
10. Klbig K, Mignaco J, Remiddi E. On nielsen's generalized polylogarithms and their numerical calculation. *BIT Numerical Mathematics* 1970; **10**(1):38–73.
11. Vepštas L. An efficient algorithm for accelerating the convergence of oscillatory series, useful for computing the polylogarithm and hurwitz zeta functions. *Numerical Algorithms* 2008; **47**(3):211–252.
12. Kormanyos C. Algorithm 910: A portable c++ multiple-precision system for special-function calculations. *ACM Trans. Math. Softw.* Feb 2011; **37**(4):45:1–45:27.
13. Bathe K. *Finite Element Procedures*. Prentice-Hall: Upper Saddle River, New Jersey, U.S.A., 1996.